

Importance of exchange-anisotropy and superexchange for the spin-state transitions in LnCoO_3 ($\text{Ln}=\text{La}, \text{Y}, \text{RE}$) cobaltates

Guoren Zhang,¹ Evgeny Gorelov,¹ Erik Koch,^{2,3} and Eva Pavarini^{1,3}

¹ *Institute for Advanced Simulation, Forschungszentrum Jülich, D-52425 Jülich, Germany*

² *German School for Simulation Sciences, 52425 Jülich, Germany*

³ *JARA High-Performance Computing*

Spin-state transitions are the hallmark of rare-earth cobaltates. In order to understand them, it is essential to identify all relevant parameters which shift the energy balance between spin states, and determine their trends. We find that Δ , the e_g - t_{2g} crystal-field splitting, increases by ~ 250 meV when increasing pressure to 8 GPa and by about 150 meV when cooling from 1000 K to 5 K. It changes, however, by less than 100 meV when La is substituted with another rare earth. Also the Hund's rule coupling \mathcal{J}_{avg} is about the same in systems with very different spin-state transition temperature, like LaCoO_3 and EuCoO_3 . Consequently, in addition to Δ and \mathcal{J}_{avg} , the Coulomb-exchange anisotropy $\Delta\mathcal{J}_{\text{avg}}$ and the super-exchange energy-gain ΔE_{SE} play a crucial role, and are comparable with spin-state dependent relaxation effects due to covalency. We show that in the LnCoO_3 series, with $\text{Ln}=\text{Y}$ or a rare earth (RE), super-exchange progressively stabilizes a low-spin ground state as the Ln^{3+} ionic radius decreases. We give a simple model to describe spin-state transitions and show that, at low temperature, the formation of isolated high-spin/low-spin pairs is favored, while in the high-temperature phase, the most likely homogeneous state is high-spin, rather than intermediate spin. An *orbital-selective* Mott state could be a fingerprint of such a state.

PACS numbers: 71.27.+a, 71.30.+h, 72.80.Ga, 71.10.-w, 71.20.-b, 75.40.Mg

I. INTRODUCTION

The nature of the spin-state transitions in LaCoO_3 (Fig. 1) is the subject of controversy for decades.^{1–20} LaCoO_3 undergoes two electronic crossovers, at $T_{\text{SS}} \sim 50 - 100$ K and $T_{\text{IM}} \sim 500 - 600$ K; the first is commonly ascribed to a change in spin-state, while the second to an insulator to metal transition.^{2,6} There is a general agreement that the ground state of LaCoO_3 is insulating and non-magnetic, with Co in the low-spin (LS) t_{2g}^6 state. The core of the debate is whether the $t_{2g}^4 e_g^2$ high-spin (HS) state^{1–5} ($S=2$), or the $t_{2g}^5 e_g^1$ intermediate-spin (IS) state^{9–15} ($S=1$) is thermally excited right above T_{SS} , and if the spin-state crossover involves two or more steps between T_{SS} and T_{IM} . Various mixed phases^{16,17} and spin-state superlattices^{18–21} have been suggested as final or intermediate step. For the high-temperature phase, a pure IS state has been proposed based on LDA+ U results¹⁷ or phenomenological thermodynamic analysis.²² To date, the controversy remains open.

Spin-state transitions have also been reported in LaCoO_3 under pressure,^{23–26} as well as in several LnCoO_3 perovskites, where Ln is Y or a rare earth (RE) heavier than La.^{27–29} In the LnCoO_3 series, the spin-state and, to a smaller extent, the insulator to metal transition, shifts to higher temperatures with decreasing RE^{3+} ionic radius.^{27–30} Since HS and IS states are Jahn-Teller (JT) active, one might expect co-operative JT distortions in correspondence with the spin-state transition. Remarkably, early neutrons diffraction data^{31–33} indicate that the structure of LaCoO_3 is rhombohedral (space group $R\bar{3}c$) with no co-operative JT distortion at all,^{5,31–33} while more recently a co-operative JT distor-

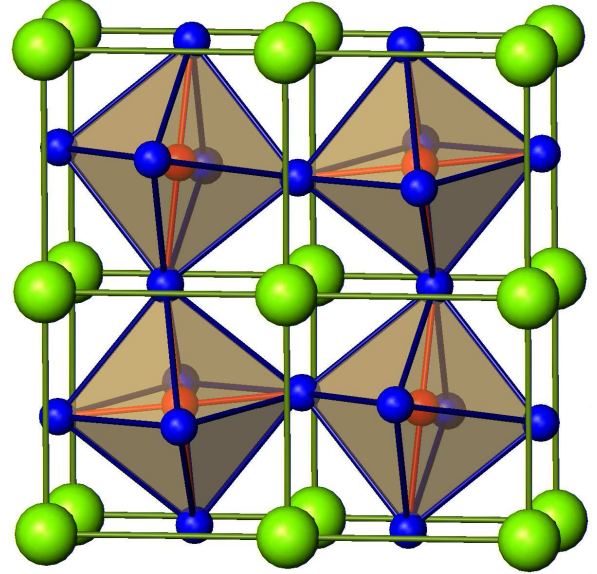


FIG. 1: (Color on-line) Rhombohedral structure of LaCoO_3 . We define the \mathbf{x} , \mathbf{y} , \mathbf{z} pseudo-cubic axes as those connecting the Co atoms; \mathbf{z} is the vertical axis, \mathbf{y} the horizontal axis, and \mathbf{x} is perpendicular to the plane of the figure.

tion (space group $I2/a$) has been found via single-crystal X-ray diffraction.^{14,34} The presence of local JT distortions is as controversial.^{5,35} On the other hand, LnCoO_3 perovskites with $\text{Ln} \neq \text{La}$ are orthorhombic (space group $Pbnm$) and do exhibit a small, weakly temperature dependent, JT distortion.^{27,28,30}

The LS \rightarrow IS scenario⁹ was popularized by total-energy LDA+ U calculations,¹² which show that for rhombohe-

dral LaCoO₃ the homogeneous IS state is almost degenerate with the LS ground state, and sizably lower in energy than the HS state.^{12,17–19} The LS→IS scenario has been used to interpret experiments pointing to a spin triplet.^{11,14,28} However, a triplet can also arise from the splitting of the HS state via spin-orbit interaction.^{13,36,37} Furthermore, it has been shown with LDA+*U* and unrestricted Hartree-Fock that some inhomogeneous LS/HS phases and/or superlattices,^{17–19} are more stable than the homogeneous IS state. Experimentally, neither the HS+LS nor other superlattices have been reported so far; instead, there are strong indications that X-ray absorption spectroscopy (XAS) and magnetic circular dichroism (MCD) data³ as well as inelastic neutron scattering experiments⁴ are compatible with a mixed HS/LS phase. It has been pointed out that the lattice could play a crucial role in such mixed phases, by expanding around HS ions due to covalency effects^{1,3,22}

While the experimental evidence in favor of LS → HS crossover at T_{SS} , perhaps with disorder phenomena, is growing,^{3,4,11} the actual parameters which tip the energy balance in favor of a given spin-state in the real materials have not been fully identified, and, to the best of our knowledge no systematic attempt to determine their evolution in the LnCoO₃ series exist. Furthermore, the interplay between spin-state and insulator to metal transition, even in the simplest homogeneous scenarios, and the nature of the high-temperature metallic phase, are not fully understood.

In the present work, we study the electronic structure trends of the LnCoO₃ family and identify the material-dependent parameters responsible for the spin-state transitions. We show that, for realistic Coulomb and exchange parameters, an IS homogeneous phase is very unlikely in any of the considered materials, both at low and high temperature. We show that, besides the interplay of the e_g - t_{2g} crystal-field Δ and the Coulomb exchange \mathcal{J}_{avg} , the exchange anisotropy $\Delta\mathcal{J}_{avg}$ and the super-exchange energy gain Δ_{SE} stabilize the LS ground state. Our results support a scenario in which HS-LS pairs, the formation of which is favored by both super-exchange interaction and covalency effects, are excited at T_{SS} . We find that, for all known experimental structures, the Jahn-Teller crystal-field splitting is weak. In the high-temperature regime, we find, within a homogeneous scenario, a HS state; in such a state, the insulator-to-metal transition depends mostly on the t_{2g} degrees of freedom. Our results could be used to distinguish a pure high-temperature HS state from a mixed HS/LS state.

II. METHOD

We calculate the electronic structure using two *ab-initio* approaches based on density-functional theory in the local-density approximation (LDA). The first is the Linear Augmented Plane Wave (LAPW) method as implemented in the Wien2k code;³⁸ to obtain hopping in-

tegrals and crystal-field splitting we use maximally localized Wannier functions.³⁹ The second approach is the downfolding technique based on the *N*th-Order Muffin-Tin Orbital (NMTO) method in the form discussed in Refs. 40. By means of these two methods, we construct the generalized Hubbard model for the Co *d* bands

$$H = - \sum_{im,i'm'\sigma} t_{m,m'}^{i,i'} c_{im\sigma}^\dagger c_{i'm'\sigma} + \frac{1}{2} \sum_{i\sigma,\sigma'} \sum_{mm'} \sum_{pp'} U_{mpm'p'} c_{im\sigma}^\dagger c_{ip\sigma'}^\dagger c_{i'p'\sigma'} c_{im'\sigma}. \quad (1)$$

Here $c_{im\sigma}^\dagger$ creates an electron with spin σ in the Wannier orbital m at site i ($m = xz, yz, xy, x^2 - y^2, 3z^2 - r^2$). $U_{mpm'p'}$ are rotationally invariant screened Coulomb integrals. The parameters $U_{mpm'p'}$ can all be expressed as a function of the (screened) Slater integrals F_0 , F_2 and F_4 . We adopt the common definition for the average direct and exchange couplings, $U_{avg} = F_0$, and $\mathcal{J}_{avg} = \frac{1}{14}(F_2 + F_4)$. A pedagogical derivation of the rotationally invariant Coulomb matrix can be found, e.g., in Ref. 41. Apart from the average exchange interaction, the exchange anisotropy plays a significant role. It is therefore convenient to express all parameters as linear combinations of U_{avg} , $\mathcal{J}_{avg} = \frac{5}{7}U_{avg}$, and $\Delta\mathcal{J}_{avg} = \mathcal{J}_{avg}(\frac{1}{5} - \frac{1}{9}\frac{F_4}{F_2})/(1 + \frac{F_4}{F_2})$; the latter measures the anisotropy in the exchange interactions. The exchange parameters for the t_{2g} and e_g states are then $J_{t_{2g}} = \mathcal{J}_{avg} + \Delta\mathcal{J}_{avg}$ and $J_{e_g} = \mathcal{J}_{avg} + 3\Delta\mathcal{J}_{avg}$, respectively; the Coulomb exchange parameters between e_g and t_{2g} states are $J_{3z^2-r^2,xz} = J_{3z^2-r^2,yz} = \mathcal{J}_{avg} - 3\Delta\mathcal{J}_{avg}$, $J_{x^2-y^2,xy} = \mathcal{J}_{avg} - 5\Delta\mathcal{J}_{avg}$, $J_{3z^2-r^2,xy} = J_{e_g}$, and $J_{x^2-y^2,xz} = J_{x^2-y^2,yz} = J_{t_{2g}}$; the orbital-diagonal direct exchange is $U_0 = U_{avg} + \frac{8}{5}\mathcal{J}_{avg}$. For some materials, we calculate the screened Coulomb integrals U_{avg} and \mathcal{J}_{avg} using the constrained local-density approximation (cLDA) approach.⁴²

We solve Hamiltonian (1) using different approaches. In section III.A we present exact diagonalization results (atomic limit). In section III.B we show results obtained with second-order perturbation theory (super-exchange energy gain). In section III.C we present dynamical mean-field theory calculations within the LDA+DMFT (local-density approximation + dynamical mean-field theory) approach; for the latter we use a weak-coupling continuous-time quantum Monte Carlo⁴³ (CT-QMC) quantum-impurity solver and work with the full self-energy matrix in orbital space,^{40,44} as discussed in Ref. 45. We obtain the spectral-function matrix by means of stochastic reconstruction.⁴⁶ Since LDA+DMFT calculations for a 5-band model with full Coulomb vertex⁴⁷ and self-energy matrix are computationally very expensive, a massively-parallel implementation as presented in Ref. 45 is essential. Structural data for LaCoO₃ are taken from Refs. 32,34, for YCoO₃ from Refs. 27, and for the other LnCoO₃ materials⁴⁸ from Refs. 28,29,49. High-pressure data are from Ref. 23.

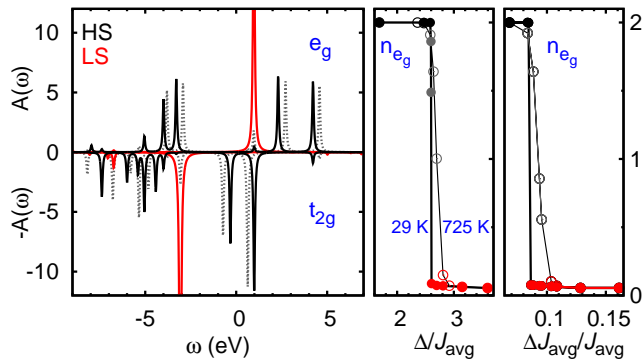


FIG. 2: (Color on-line) Left: Atomic spectral-functions at 29 K for different values of the ratio $\Delta/\mathcal{J}_{\text{avg}}$. Full line, dark: $\Delta/\mathcal{J}_{\text{avg}} \sim 1.69$. Dotted line: $\Delta/\mathcal{J}_{\text{avg}} \sim 2.60$. Full line, light: $\Delta/\mathcal{J}_{\text{avg}} \sim 2.61$. Coulomb parameters: $U_{\text{avg}} = 3$ eV, $\mathcal{J}_{\text{avg}} = 0.89$ eV. Center: occupation of the e_g states as a function of $\Delta/\mathcal{J}_{\text{avg}}$ at low and high temperature. Right: occupation of the e_g states as a function of $\Delta\mathcal{J}_{\text{avg}}/\mathcal{J}_{\text{avg}}$ at low and high temperature; the results are obtained for $\mathcal{J}_{\text{avg}} \sim 0.89$ eV, $\Delta/\mathcal{J}_{\text{avg}} \sim 2.64$ and varying F_4/F_2 in the interval $[0.1, 0.8]$.

III. RESULTS

A. Atomic limit, Jahn-Teller, and constraints

Let us examine the eigenstates of (1) in the atomic limit, i.e., in the limit $t_{m,m'}^{i,i'} = 0$ for $i \neq i'$ (see Fig. 2). The crystal-field states, the states which diagonalize the on-site matrix $t_{m,m'}^{i,i}$, have energy ε_α , with $\varepsilon_\alpha \leq \varepsilon_{\alpha+1}$; $\alpha = 1, 2, 3$ are t_{2g} -like states and $\alpha = 4, 5$ e_g -like. In the atomic limit, the energy of the low-spin state (t_{2g}^6) is

$$E_L \sim 15U_0 - 30(\mathcal{J}_{\text{avg}} + \Delta\mathcal{J}_{\text{avg}}) + 2 \sum_{\alpha \in t_{2g}} \varepsilon_\alpha.$$

The states with intermediate spin ($t_{2g}^5 e_g^1$) can be written as $|\underline{\alpha}, \beta\rangle$, where α is the t_{2g} hole orbital and β the e_g electron orbital. The energy of the IS, in the limit in which only the density-density Coulomb terms contribute, is

$$E_I \sim E_L - 3\mathcal{J}_{\text{avg}} + (23 + f)\Delta\mathcal{J}_{\text{avg}} + \Delta^{\text{LI}},$$

where $\Delta^{\text{LI}} = \varepsilon_4 - \varepsilon_3$; the factor f yields the deviation from the average anisotropy of the exchange interaction; $f = -8$ for $|\underline{xy}, x^2 - y^2\rangle$ and cyclic xyz permutations. The energy of a high-spin $t_{2g}^4 e_g^2$ is

$$E_H \sim E_L - 8\mathcal{J}_{\text{avg}} + 30\Delta\mathcal{J}_{\text{avg}} + 2\Delta^{\text{LH}},$$

where $\Delta^{\text{LH}} = (\varepsilon_5 + \varepsilon_4 - \varepsilon_3 - \varepsilon_2)/2$. From energy differences between spin configurations we can obtain constraints for the parameters. Theoretical estimates⁵⁰ yield $F_2 \sim 10.64$ eV and $F_4 \sim 6.8$ eV; with these values $\mathcal{J}_{\text{avg}} \sim 0.89$ eV, and $\Delta\mathcal{J}_{\text{avg}} \sim 0.07$ eV $\sim 0.08\mathcal{J}_{\text{avg}}$; other estimates⁵¹ yield slightly smaller values; by using cLDA we obtain $\mathcal{J}_{\text{avg}} \sim 0.7$ eV; furthermore, we

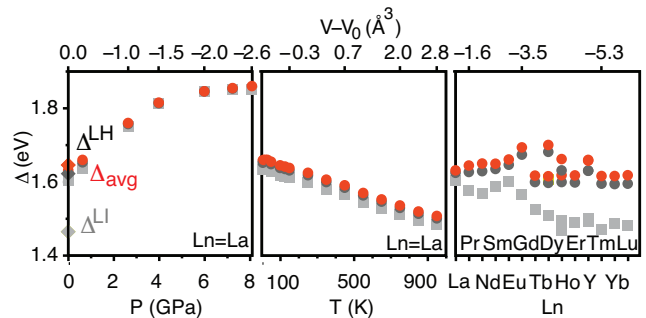


FIG. 3: (Color on-line) Crystal-field splittings as a function of pressure (left), temperature (center), and of Ln ion (right). The corresponding volumes are also given; V_0 is the volume of LaCoO_3 at room temperature and ambient pressure. $\Delta^{\text{LI}} = \varepsilon_4 - \varepsilon_3$ (squares), $\Delta_{\text{avg}} = (\varepsilon_4 + \varepsilon_5)/2 - (\varepsilon_1 + \varepsilon_2 + \varepsilon_3)/3$ (dark circles), and $\Delta^{\text{LH}} = (\varepsilon_4 + \varepsilon_5)/2 - (\varepsilon_2 + \varepsilon_3)/2$ (light circles) are shown. In the cubic limit, $\Delta^{\text{LI}} = \Delta^{\text{LH}} = \Delta_{\text{avg}} = \Delta$. Multiple points for the same compound are results from different structural data sets.

find that \mathcal{J}_{avg} varies little when La is replaced by Eu in EuCoO_3 , a material which apparently exhibits no spin-state transition below the insulator-to-metal transition.²⁹ Since screened Coulomb exchange parameters can only be obtained within given approximations, we will discuss our results for a range of plausible values of \mathcal{J}_{avg} , ranging from 0.5 eV to 1 eV.

In Fig. 3 we show the calculated crystal-field splitting. We calculate the splittings in LaCoO_3 at ambient pressure and for increasing temperature,^{31,32} at room temperature for increasing pressure^{23-26,52} and in the series of RECoO_3 compounds.^{27,49,53,54} Our results show that $\Delta^{\text{LH}} \sim 1.6 - 1.7$ eV in the full series,⁵⁵ while $\Delta^{\text{LI}} \sim 1.4 - 1.6$ eV. From these results we can derive the following conclusions. The ground state is LS if these conditions are met

$$\begin{aligned} \Delta^{\text{LH}} &\gtrsim 4\mathcal{J}_{\text{avg}} - 15\Delta\mathcal{J}_{\text{avg}} \sim 2.8\mathcal{J}_{\text{avg}}, \\ \Delta^{\text{LI}} &\gtrsim 3\mathcal{J}_{\text{avg}} - (23 + f)\Delta\mathcal{J}_{\text{avg}} \sim 1.16-1.8\mathcal{J}_{\text{avg}}, \end{aligned}$$

where for the second condition we give the range varying f from 0 (average) to -8 ($|\underline{xy}, x^2 - y^2\rangle$). Let us consider the cubic case ($\Delta^{\text{LH}} = \Delta^{\text{LI}} = \Delta_{\text{avg}} = \Delta$). In this case, the first condition is the most stringent. Exact diagonalization of the atomic limit Hamiltonian with full exchange interaction and $\Delta\mathcal{J}_{\text{avg}}/\mathcal{J}_{\text{avg}} \sim 0.08$ (Fig. 2) indeed leads to a switch between a high and low spin ground state at slightly smaller values, $\Delta \sim 2.6\mathcal{J}_{\text{avg}}$. From these results we conclude that, to explain a $S = 0$ ground state in the atomic limit, \mathcal{J}_{avg} must be slightly smaller than estimated with cLDA and similar approaches, $\mathcal{J}_{\text{avg}} \sim 0.6$ eV; alternatively, less likely, $\mathcal{J}_{\text{avg}} \sim 0.7$ eV but the anisotropy should be sizably larger than in the free atom,⁵⁶ $\Delta\mathcal{J}_{\text{avg}} \sim 0.12\mathcal{J}_{\text{avg}}$. In any case, with the crystal field splittings in Fig. 3, we are quite close to the HS/LS crossover. In this parameter region, the ~ 100 - 200 meV changes in crystal-field that we find

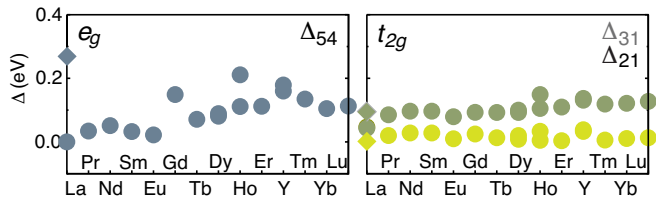


FIG. 4: (Color on-line) Crystal-field splitting (in eV) of e_g (left) and t_{2g} (right) states at room temperature as a function of decreasing ionic radius. Multiple points for the same compound are results from different structural data.^{27,49,53,54,58} LaCoO_3 : $I2/a$ (diamonds) and $R\bar{3}c$ (circles).

(Fig. 3) with increasing temperature or pressure could indeed explain *alone* a spin-state crossover from LS to HS or viceversa. For a IS ground state, the following conditions should be met

$$2\Delta^{\text{LH}} - \Delta^{\text{LI}} \gtrsim \left(5 - (7 - f) \frac{\Delta\mathcal{J}_{\text{avg}}}{\mathcal{J}_{\text{avg}}}\right) \mathcal{J}_{\text{avg}} \sim 4.5\text{-}3.8\mathcal{J}_{\text{avg}}$$

$$\Delta^{\text{LI}} \leq 3\mathcal{J}_{\text{avg}} - (23 + f)\Delta\mathcal{J}_{\text{avg}} \sim 1.16\text{-}1.8\mathcal{J}_{\text{avg}}$$

This definitely excludes a IS ground state in the cubic case as, in all systems considered, the two conditions are never satisfied at the same time. For a $\text{LS} \rightarrow \text{IS}$ scenario, it could be however sufficient that the IS state is lower than the HS (first condition). In the cubic case, for the parameters in Fig. 3, this could happen only for apparently unrealistically small Coulomb exchange \mathcal{J}_{avg} (~ 0.4 eV or smaller) or unrealistically large⁵⁶ anisotropy $\Delta\mathcal{J}_{\text{avg}}/\mathcal{J}_{\text{avg}}$ (~ 0.16); in these cases the IS would, however, be quite high in energy (~ 1 eV or more) above the LS. Thus the predictions of conventional ligand-field theory⁵⁷ are in agreement with our results for the atomic limit.

Let us analyze the effects of crystal distortions on the crystal-field splittings of e_g ($\Delta_{54} = \varepsilon_5 - \varepsilon_4$) and t_{2g} ($\Delta_{31} = \varepsilon_3 - \varepsilon_1$, $\Delta_{21} = \varepsilon_2 - \varepsilon_1$) states, and the corresponding crystal-field orbitals. In Fig. 4 we show Δ_{54} , Δ_{31} and Δ_{21} along the series; we find that the splitting of e_g states, Δ_{54} , reaches a maximum of 200 meV in HoCoO_3 , and 250 meV in tetragonal³⁴ LaCoO_3 , and is zero in rhombohedral LaCoO_3 ; furthermore, we find that Δ_{21} is small while Δ_{54} and Δ_{31} are comparable, the only exception being the $I2/a$ LaCoO_3 structure; finally, across the spin-state transition, for available structural data, we find either basically no change in e_g and t_{2g} crystal-field splittings (LaCoO_3 , $R\bar{3}c$) or a tiny change of 40 meV and no significant change in occupied orbital (YCoO_3). Even if we assume that the crystal-field splittings in Fig. 4 are completely ascribed to the Jahn-Teller effect, they are small compared to Jahn-Teller systems such as manganites or cuprates;⁴⁴ they are comparable with splittings arising from the GdFeO_3 -type distortion ($Pbnm$ structures)^{40,59} which progressively increase along the LnCoO_3 series.^{53,54} LaCoO_3 has to be discussed

separately. While the presence of JT distortion is still controversial experimentally, even the monoclinic structure with co-operative Jahn-Teller distortion reported in Ref. 34 leads to a small splitting of e_g and t_{2g} states (see Fig. 4), although larger than for all other LnCoO_3 compounds considered here.

The splittings of e_g and t_{2g} states might affect the energy balance between spin states. To quantify this effect, we introduce the average splitting $\delta\Delta = (\Delta_{54} + \Delta_{31})/2$. Then, on the basis of Fig. 4, $\Delta^{\text{LH}} \sim \Delta$, $\Delta^{\text{LI}} \sim \Delta - \delta\Delta$. In the light of presently known structural data, remarkably, in the full LnCoO_3 series, $\delta\Delta$ is at most 150 meV, which is insufficient to lead to a LS-IS scenario, which would require $\delta\Delta \sim 1\text{-}1.7 \mathcal{J}_{\text{avg}}$ or larger. Such a scenario could perhaps start to play a role under high pressure, if $\delta\Delta$ sizably increases.

Our results show that the anisotropy $\Delta\mathcal{J}_{\text{avg}}$ plays an important role in stabilizing the low-spin ground state (Fig. 2); if we neglect it ($\mathcal{J}_1 = \mathcal{J}_{\text{avg}} = \mathcal{J}$), an approximation often adopted, the constraint for a low spin ground state becomes $\Delta^{\text{LH}} > 4\mathcal{J}$. Thus, if the e_g - t_{2g} crystal-field splitting Δ has the values of Δ_{avg} in Fig. 3, the effective Coulomb exchange has to be as small as $\mathcal{J} \sim 0.4$ eV in order to obtain a LS ground state. On the other hand, if the anisotropy is unrealistically larger than for atomic orbitals, the IS state can become the first excited state. As a consequence, for systems close to spin-state transitions, differences in total energy between spin states might be extremely sensitive to the approximations adopted in describing the multiplet structure.^{60,61}

The value of U_{avg} does not affect the energy differences between spin-states in the atomic limit, but is relevant for the insulator to metal transition and the gap, as well as for super-exchange. Theoretical estimates based on density-functional theory^{12,50,62} yield ~ 8 eV in LaCoO_3 , and we find similar values with constrained LDA. Experimental estimates based on electron spectroscopy⁶³ yield sizably smaller values (~ 3.5 eV); similar values were adopted in many works.^{17,19,37} A configuration-interaction cluster model analysis of spectroscopic data yields $U_{\text{avg}} = 5.5$ eV for the low and intermediate spin-state and ~ 6.8 eV for the high-spin state. Since the value of U_{avg} affects energy scales such as the size of the gap and super-exchange, when necessary, in the next sections, we present results for several U_{avg} .

In conclusion, our results show that, in the atomic limit, for all systems analyzed, a $\text{LS} \rightarrow \text{IS}$ scenario is unlikely. At close inspection, LDA+ U total-energy calculations are in line with this conclusion,^{12,17-19} as they indicate clearly that the stabilization of a given local magnetic state (IS or HS) strongly depends on the number and type of surrounding magnetic neighbors, suggesting that co-operative, band, or at least multi-site effects play a crucial role; at low concentrations, in the absence of magnetic neighbors, the HS appears to be the favored magnetic state.^{1,17} Another important aspect is the evolution of the parameters with increasing temperature. For LaCoO_3 we find that the crystal-field Δ_{avg} is re-

duced by about 150 meV when the temperature increases from 5 K to 1000 K. Remarkably, magnetic susceptibility data¹¹ indicate that the LS→ HS activation energy, Δ_{AE} , increases with temperature; similarly, the analysis of XAS data by means of the truncated configuration-interaction cluster approach³ suggests a rise of about 60 meV from 50 K to 700 K.¹¹ This result cannot be explained in the atomic limit, even including the effects of spin-orbit interaction, $\lambda \mathbf{S} \cdot \mathbf{L}$; we calculate the spin-orbit coupling λ for LaCoO_3 and find $\lambda \sim 54$ meV, slightly larger than the one assumed in model calculations,³⁶ but too small to affect the trends on Δ_{avg} . Our results also exclude that the rhombohedral distortions increase enough with temperature to overcome the decrease in Δ_{avg} due to the increasing volume.⁶⁴

B. Super exchange

Away from the atomic limit, super-exchange affects the energy balance. However, is the super-exchange energy gain large enough to be relevant in the spin-state crossover at T_{SS} ? In this section we calculate the super-exchange energy gain for several types of Co-Co bonds: LS-LS, HS-HS and LS-HS pairs; we do not consider IS-LS pairs, whose formation at low temperature is unlikely.¹⁷ While differences in the energy of multiplets with fixed number of electrons, relevant to determine the spin-state, are of the order \mathcal{J} , virtual excitations of electrons to neighboring sites, relevant for super-exchange, involve the direct Coulomb energy \mathcal{U} . Thus Coulomb exchange anisotropy $\Delta \mathcal{J}_{\text{avg}}$ has a small effect on super-exchange; for simplicity we neglect it and consider density-density terms only. For a LS-LS pair we obtain the energy gain

$$\Delta E_{\text{SE}}^{\text{LS-LS}} = - \sum_{\alpha=1}^3 \sum_{\alpha'=4}^5 \frac{|t_{\alpha',\alpha}^{i,i'}|^2 + |t_{\alpha,\alpha'}^{i,i'}|^2}{U_0 - 5\mathcal{J} + \Delta_{\alpha',\alpha}}, \quad (2)$$

where $\Delta_{\alpha',\alpha} = \varepsilon_{\alpha'} - \varepsilon_{\alpha}$. For a HS-HS pair, assuming that Co ions are in a paramagnetic state, we obtain

$$\Delta E_{\text{SE}}^{\text{HS-HS}} = -\frac{1}{2n_{\beta}^2} \sum_{\{\beta\},\{\beta'\}} \left[\sum_{\alpha \neq \beta} \sum_{\alpha' \neq \beta'} \frac{|t_{\alpha,\alpha'}^{i,i'}|^2 + |t_{\alpha',\alpha}^{i,i'}|^2}{U_0 + 3\mathcal{J} + \Delta_{\alpha',\alpha}} \right. \\ \left. + \sum_{\alpha' \neq \beta'} \frac{|t_{\beta,\alpha'}^{i,i'}|^2 + |t_{\alpha',\beta}^{i,i'}|^2}{U_0 - 3\mathcal{J} + \Delta_{\alpha',\beta}} + \frac{|t_{\beta,\alpha'}^{i,i'}|^2 + |t_{\alpha',\beta}^{i,i'}|^2}{U_0 + \mathcal{J} + \Delta_{\alpha',\beta}} \right],$$

where $\{\beta\}$ are the n_{β} degenerate t_{2g} levels, over which we average. Results for material-dependent hopping integrals are shown in Fig. 5. We find that for $U_{\text{avg}} \sim 5$ eV or larger the energy gains do not change much with increasing \mathcal{J} from 0 to 1 eV.⁶⁵ Instead, for fixed $\mathcal{J} \sim 0.89$ eV, we find a remarkable change in $\Delta E_{\text{SE}}^{\text{LS-LS}}$ reducing U_{avg} to ~ 3.5 eV, because the denominator sizably decrease. In Fig. 5 we show two significant parameter ranges. For $U_{\text{avg}} \sim 5.5$ eV, super-exchange favors a high-spin ground

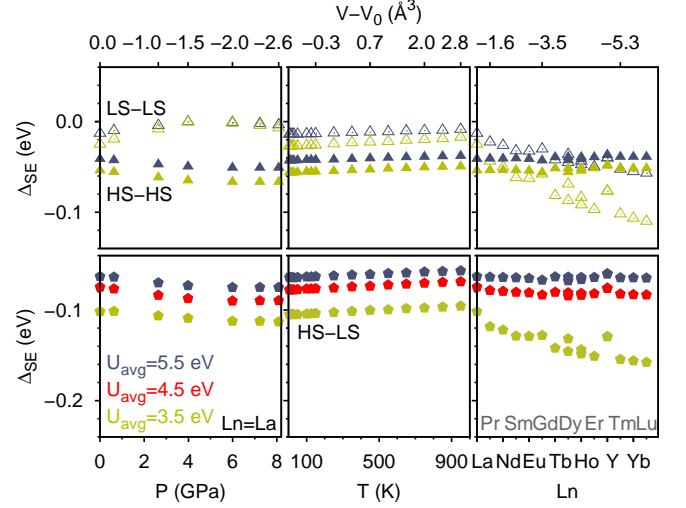


FIG. 5: (Color on-line) Super-exchange energy gain per bond, Δ_{SE} , for a LS-LS pair (empty triangles), a HS-HS pair (filled triangles) and a LS-HS pair (pentagons). Left: Δ_{SE} as a function of pressure. Center: Δ_{SE} as a function of temperature. Right: Δ_{SE} as a function of Ln ion. The corresponding volumes are also given; V_0 is the volume of LaCoO_3 at room temperature and ambient pressure. Multiple points for the same compound are results from different structural data sets.

state for LaCoO_3 for all temperature and pressures considered. In the series LnCoO_3 , the super-exchange energy gain becomes larger for a LS ground state for ions smaller than Dy^{3+} . For $U_{\text{avg}} \sim 3.5$ eV the crossing happens already for $\text{Ln}=\text{Sm}$, and the energy gain per LS-LS bond increases sizably to 90 meV around $\text{Ln}=\text{Y}$.

It is at this point crucial to evaluate also the super-exchange energy gain associated with the formation of a HS-LS bond, given by

$$\Delta E_{\text{SE}}^{\text{HS-LS}} = -\frac{1}{2n_{\beta}} \sum_{\{\beta\}} \left[\sum_{\alpha \neq \beta} \sum_{\alpha'=4}^5 \frac{|t_{\alpha,\alpha'}^{i,i'}|^2 + |t_{\alpha',\alpha}^{i,i'}|^2}{U_0 - \mathcal{J} + \Delta_{\alpha',\alpha}} \right. \\ \left. + \sum_{\alpha'=4}^5 \left(\frac{|t_{\beta,\alpha'}^{i,i'}|^2 + |t_{\alpha',\beta}^{i,i'}|^2}{U_0 - 7\mathcal{J} + \Delta_{\alpha',\beta}} + \frac{|t_{\beta,\alpha'}^{i,i'}|^2 + |t_{\alpha',\beta}^{i,i'}|^2}{U_0 - 3\mathcal{J} + \Delta_{\alpha',\beta}} \right) \right. \\ \left. + \sum_{\alpha' \neq \beta} \sum_{\alpha=1}^3 \frac{|t_{\alpha,\alpha'}^{i,i'}|^2 + |t_{\alpha',\alpha}^{i,i'}|^2}{U_0 - \mathcal{J} + \Delta_{\alpha',\alpha}} \right]. \quad (3)$$

This energy gain is relevant in many scenarios of spin-state crossover. We find that $\Delta E_{\text{SE}}^{\text{HS-LS}}/\Delta E_{\text{SE}}^{\text{HS-HS}}$ is ~ 1.5 -2 for $U_{\text{avg}} \sim 5.5$, and it increases with decreasing U_{avg} . Furthermore, all super-exchange energy gains calculated here vary slowly with increasing temperature. These results show that, even neglecting lattice relaxation effects,¹ it is energetically favorable to form isolated HS ions rather than HS-HS bonds.

The super-exchange energy difference between a HS-

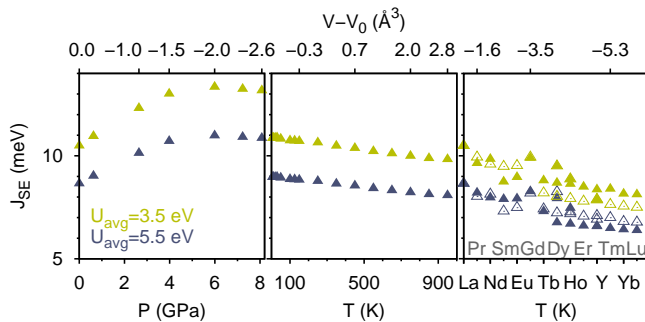


FIG. 6: (Color on-line) Magnetic coupling J_{SE} for a HS-HS pair, as a function of pressure (left), temperature (center), and of Ln ion (right; empty symbols: (001) direction; filled symbols: (100) or (010) direction). The corresponding volumes are also given; V_0 is the volume of LaCoO_3 at room temperature and ambient pressure. Multiple points for the same compound are results from different structural data sets.

HS and a LS-LS pair is

$$\delta E^{LH} = (\Delta_{SE}^{\text{HS-HS}} - \Delta_{SE}^{\text{LS-LS}}).$$

For $U_{\text{avg}} = 5.5$ eV, we find $\delta E^{LH} < 0$ (energy gain if a HS-HS is formed) for systems with larger ionic radius and $\delta E^{LH} > 0$ (energy loss) for systems with smaller ionic radius. The energy cost of a HS-HS pair with respect to two isolated HS ions is

$$\delta \Delta_{SE} \sim \Delta_{SE}^{\text{HS-HS}} + \Delta_{SE}^{\text{LS-LS}} - 2\Delta_{SE}^{\text{HS-LS}}.$$

We find that $\delta \Delta_{SE} > 0$ for all systems and all parameter ranges. For $U_{\text{avg}} = 5.5$ eV, it decreases from 70 to 30 meV along the series; for fixed Ln, it increases with decreasing U_{avg} . Based on these results, we can build a model which describes the system. We introduce pseudospin operators σ_z , and identify LS sites with spin down and HS sites with spin up.⁶⁶ The interactions between spins yield a Ising-like model

$$H_{\text{eff}} = \sum_i h(T) \sigma_z^i + \frac{1}{2} \sum_{\langle ji \rangle} J \sigma_z^i \sigma_z^j.$$

Here $n_i = n_i^H + n_i^L = 1$ is the occupation per site, $\sigma_z^i = n_i^H - n_i^L$, and $\langle ji \rangle$ are near neighboring lattice sites. The parameter

$$h(T) = \frac{1}{2} E^{\text{LH}}(T) + \frac{1}{4} q \delta E^{\text{LH}},$$

where q is the coordination number, plays the role of an external field. The temperature enters explicitly only in

$$E^{\text{LH}}(T) = -3\mathcal{J}_{\text{avg}} + 30\Delta\mathcal{J}_{\text{avg}} + 2\Delta^{\text{LH}}(T)$$

The coupling is $J = \frac{1}{4} \delta \Delta_{SE} > 0$ (antiferro). In static mean-field a LS homogeneous state is given by the solution of the self-consistent equation

$$\langle \sigma_z^i \rangle = \tanh(-h(T) - qJ \langle \sigma_z^i \rangle) \beta.$$

At low temperature $h(T) > 0$ is large and the system is in a fully polarized ferro LS state. Increasing the temperature, $h(T)$ decreases linearly (Fig. 3) allowing the formation of some HS sites. We find that δE^{LH} increases with decreasing ionic radius; the crystal-field is instead maximum around Ln=Eu (Fig. 3). An increase of activation energy from 1200 K in LaCoO_3 to 3200 K in EuCoO_3 has been indeed reported.²⁹

When HS states form, covalency-driven lattice relaxation effects^{1,3} change the environment. In our model, if we take into account only two-sites interactions, this effect enhances $J \rightarrow J' = J + J_{\text{rel}}$, thus favoring a AF HS/LS phase, described in mean field by

$$\langle \sigma_z^i \rangle = \tanh(-h(T) + qJ' \langle \sigma_z^i \rangle) \beta.$$

An overestimate of J_{rel} can be obtained by using the difference between HS and LS in empirical ionic radii ($\delta r_{\text{IR}} \sim 0.06 \text{ \AA}$) and the fact that Δ varies linearly when changing the Co-O distance by a small amount; we can estimate the slope from our results (Fig. 3). We find $J_{\text{rel}} \sim \frac{1}{4} 2\delta\Delta$, with $2\delta\Delta \sim \frac{1}{q} 2\Delta' \delta r_{\text{IR}} \sim 90$ meV, decreasing to 80 meV at high temperatures, i.e. comparable with the super-exchange term $\delta \Delta_{SE}$.

If $h(T) = 0$, eventually an antiferro ordered HS+LS lattice forms; the critical temperature for such a state can be estimated using mean-field theory, $k_B T_{\text{HS+LS}} = qJ'$. If $J_{\text{rel}} = 0$, for $U_{\text{avg}} = 5.5$ eV $T_{\text{HS+LS}} \sim 1200$ K for Ln=La, decreasing to 500 K for Ln=Lu; J_{rel} enhances $T_{\text{HS+LS}}$ of about 1300 K.

The critical temperatures we obtain are very large. However, although $h(T) \rightarrow 0$ with increasing temperature, it likely remains comparable to J' till very high temperatures; thus the lattice stays disordered, and perhaps even close to a LS ferro solution in a large temperature range, with $\langle \sigma_z^i \rangle$ (i.e., the occupation of LS states) decreasing linearly with increasing temperature. Indeed, in LaCoO_3 it has been reported that the fraction of HS sites increasing slowly from 0.1 to 0.4 increasing the temperature from 100 to 700 K.³ Hysteresis effects could arise because of the lattice relaxation.

Up to here we have assumed that in HS-HS pairs Co HS ions stay paramagnetic and paraorbital. However, a specific molecular state could form as well as a spin singlet or triplet. We find that orbitals in the degenerate t_{2g} states play a minor role, because the energy differences of different orbital states with respect to the orbital average is small. Instead, the formation of a magnetic singlet could play a role. In order to estimate the associated energy gain, we calculated the coupling constant J_{SE} of the Heisenberg interaction $J_{SE} \mathbf{S}_i \cdot \mathbf{S}_j$ for a HS pair. We find that J_{SE} is AFM for all systems (see Fig. 6). In LaCoO_3 , for $U_{\text{avg}} = 5.5$ eV we find $J_{SE} \sim 7$ meV at room temperature and ambient pressure; it increases to 10 meV if the pressure rises to 8 GPa, and slightly decreases with increasing temperature. Reducing the ionic radius the anisotropy of J_{SE} increases, but the average magnetic coupling decreases down to 8 meV for Ln=Lu. Next we assume that in all system, due to

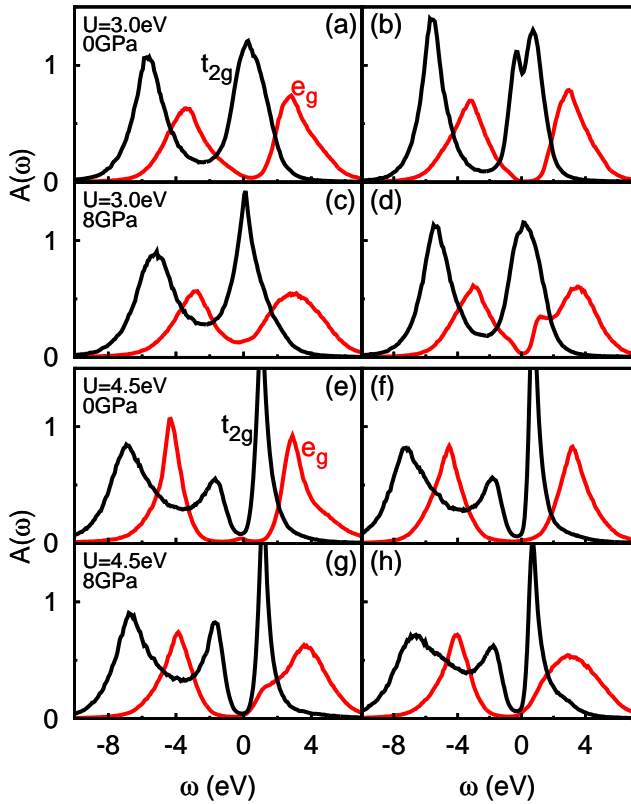


FIG. 7: (Color on-line) Orbital-resolved LDA+DMFT spectral functions (t_{2g} and e_g) of LaCoO₃ for decreasing temperature, approaching the insulator to metal transition from above ($T/T_{\text{IM}} \sim 4 \rightarrow 2$). Upper panels: $U = U_{\text{avg}} = 3$ eV, $P=0$ GPa and 8 GPa. Lower panels: $U = U_{\text{avg}} = 4.5$ eV, $P=0$ GPa and 8 GPa.

the spin-orbit coupling, the effective magnetic moment $p = \sqrt{J(J+1)} \sim \sqrt{2}$; then, the magnetic energy gain associated with the formation of a singlet is $-\frac{9}{4}J_{\text{SE}}$, which in LaCoO₃ is ~ -18 meV. This energy gain partially reduces $\delta\Delta_{\text{SE}}$ and therefore J , which would change sign around the end of the series if $U_{\text{avg}} \sim 5.5$ eV; $\delta\Delta_{\text{SE}}$ increases however rapidly with decreasing U_{avg} . The smaller $T_{\text{HS+LS}}$ the more favorable is a disordered phase, reinforcing the conclusions of the paragraph above.

However, the magnetic coupling J_{SE} is sizable, and magnetic interactions would be crucial in a homogeneous HS-HS state. In mean-field theory, the critical temperature $T_N \sim \frac{9}{4}J_{\text{SE}}J(J+1)$ should then be ~ 500 K for LaCoO₃, decreasing in the series to 400 K and increasing under pressure to about 700 K. The mean-field values are overestimates; quantum-fluctuation effects, further crystal-field splittings reducing the effective magnetic moment, and the zero-field splitting, reduce T_N . Still, even taking reduction factors into account, many cobaltates, if in a homogeneous HS state, should be magnetic because the spin-state transition occurs at $T_{\text{SS}} < T_N$; in the presence of lonely HS-HS pairs, anti-ferromagnetic short range correlations could be detected. On the other

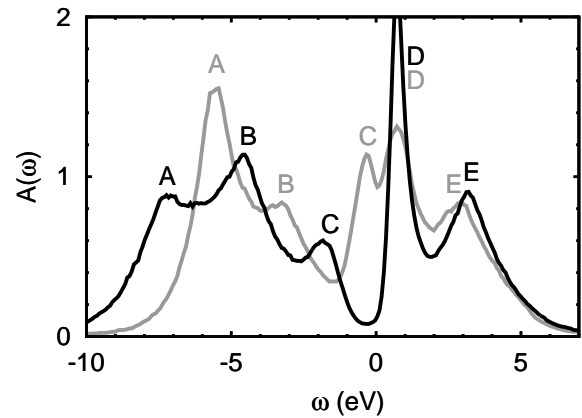


FIG. 8: Total LDA+DMFT spectral function ($T/T_{\text{IM}} \sim 3$) for LaCoO₃; $U_{\text{avg}} = 3$ eV (light) and $U_{\text{avg}} = 4.5$ eV (dark).

hand, if the number of ions thermally excited to a HS state is small till high temperature and the phase is disordered, weak FM short-range correlations, as reported in dynamic neutron-scattering experiments, could perhaps be triggered by a double-exchange like mechanism,⁵⁰ or even alone by the small but finite zero-field splitting.¹¹

C. High-temperature phase

The transition observed at T_{IM} is usually ascribed to a semiconductor-to metal transition, the nature of which is hotly debated. There are indications that strong correlations play a crucial role, and that the spin-state transition is also a crossover from a spin-gapped insulator to a Mott insulator.^{8,67} In the absence of firm evidence of the formation of superlattices, we analyze to what extent the insulator to metal transition can be understood in terms of a Mott transition within the homogeneous phase. Several works indeed suggest that the high-temperature phase could be a metallic homogeneous IS state.^{17,22} To clarify if this can be the case, we solve the Hamiltonian (1) by means of the LDA+DMFT approach;⁶⁸ we perform calculations for LaCoO₃ (Figs. 7, and 8), for which spectral properties are best known. The experimental gap is ~ 0.2 eV at low temperatures and slightly larger (~ 0.5 eV) above 300 K; to be consistent with experimental gaps, we vary U_{avg} between 3 eV and 5 eV.

Fig. 7 shows the LDA+DMFT results for $U_{\text{avg}} = 3$ eV and the ambient pressure structure for temperatures approaching T_{IM} (panels (a) and (b)). We find a homogeneous high-spin state; thus we do not find support for the proposed^{17,22} homogeneous IS state at high-temperature. Remarkably, we find metallic t_{2g} and insulating e_g spectral-functions, i.e., an *orbital-selective* Mott state. This can be understood from the fact the t_{2g} electrons have a larger orbital degeneracy,⁶⁹ although a smaller band-width (Fig.9), while the e_g electrons are half-filled in the HS state, and therefore the exchange

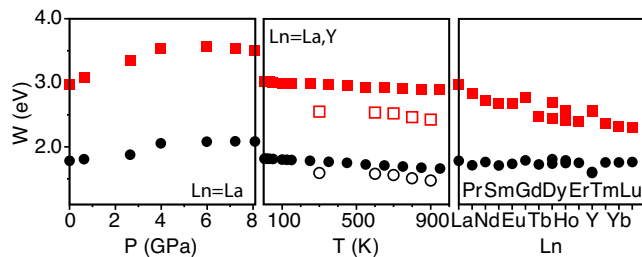


FIG. 9: (Color on-line) LnCoO_3 series: Evolution of the e_g (squares) and t_{2g} (circles) bandwidth with pressure ($\text{Ln}=\text{La}$, $R\bar{3}c$ structure), temperature (filled symbols: $\text{Ln}=\text{La}$ ($R\bar{3}c$ structure) and empty symbols: $\text{Ln}=\text{Y}$), and ionic radius Ln^{3+} (right panel).

coupling \mathcal{J}_{avg} effectively enhances the Coulomb repulsion. Decreasing the temperature towards T_{IM} a pseudo gap opens in the e_g spectral-function, and eventually an insulating regime with a small gap and a corresponding bad metal behavior appears. We find that the multiplet positions in the spectral function are close to the atomic limit high-spin curve in Fig. 2. We repeat the calculation for the 8 GPa structure (Fig. 7, panels (c) and (d)); this system has a larger crystal-field Δ_{avg} , very close, for the chosen exchange parameters, to the low spin to high-spin ground-state crossover in the atomic limit. Compared to the ambient pressure case, the e_g gap is smaller, while, at fixed temperature, the t_{2g} spectral function remains metallic with higher low-energy density of states. These results indicate that, as far as the state remains HS, at 8 GPa the insulator to metal transition should occur at lower temperature than at ambient pressure, i.e. the system should stay metallic. Experiments show however that LaCoO_3 returns to the insulating state under pressure.^{24,26} Our results exclude that this can happen in a HS scenario, and are instead compatible with the suggestion²⁴ that the metal-insulator transition observed under pressure is driven by a spin-state transition.

Increasing U_{avg} to ~ 4.5 eV we find (Fig. 7, panels (e), (f), (g), (h)) that a real gap opens in the t_{2g} spectral function, and both e_g and t_{2g} spectral functions are insulating even at high temperatures. The t_{2g} gap is small, still compatible with the bad metal behavior observed for $T > T_{\text{IM}}$. Furthermore, calculations for the high-pressure structure show that the t_{2g} spectral function does not change much while the e_g gap is reduced. This can be understood observing that the e_g band-width increases substantially more than the t_{2g} band-width increasing pressure (Fig. 9).

The total spectral function at ambient pressure is shown in Fig. 8. We find three negative energy peaks (A,B,C), and two positive energy features (D,E). For $U_{\text{avg}} \sim 4.5$ eV peak A is at -7.5 eV, peak B at -4.7 eV, ~ 2 eV above, and peak C at ~ -1.9 eV, features all observed in XPS, UPS, or photoemission data.^{10,37,63,70}

The spectra for $U_{\text{avg}}=3$ eV and $U_{\text{avg}}=4.5$ eV differ in particular in the photoemission part; reducing U_{avg} to 3 eV, we find that the spectrum is moved almost rigidly toward the right by about 2 eV; the first and second features move to -5.5 eV and -3.5 eV respectively, while the lowest energy peak moves to -0.5 eV, very close to the Fermi edge, to partially merge with the 0.8 eV peak; finally, spectral weight moves from B to C and A. While the exact positions of peaks A, B, and C shift with U_{avg} , the overall shape of the spectral function appears in line with XPS, BIS, XAS and PES data at room temperature.^{63,70,71} The positive energy features D and E at ~ 1 eV and ~ 3 eV are reflected in the form of the XAS and BIS spectra.⁶³

Thus the insulator to metal transition, as described in a homogeneous scenario, and the spin-state crossover exhibit different trends; the spin-state crossover is controlled by small changes in Δ , exchange anisotropy and super-exchange, parameters which change sizably with decreasing ionic radius. If the homogeneous HS is populated, a Mott insulator to bad metal transition can occur, at a temperature which depends strongly on the t_{2g} band-width and crystal-fields.

IV. CONCLUSIONS

We have studied the nature of the spin-state and metal-insulator transition in LnCoO_3 cobaltates. We show that a low-temperature intermediate spin-state scenario is unlikely in the full LnCoO_3 series. We show that the spin-state transition is controlled not only by the cubic crystal-field Δ and the average Coulomb exchange \mathcal{J}_{avg} but, surprisingly, also by the Coulomb exchange anisotropy $\Delta\mathcal{J}_{\text{avg}}$ and by super-exchange. We propose a simple Ising-like model to describe the spin-state transition. We find that lattice relaxation and super-exchange yield anti-ferro coupling of the same order, which compete with the crystal field. Our model qualitatively explains the trends observed in spin-state transitions in the LnCoO_3 series. By using the LDA+DMFT approach, we show that in LaCoO_3 a high-temperature homogeneous intermediate spin state is unlikely. Within a homogeneous HS state, we find that the HS metal-insulator transition has a different nature than the spin-state transition, as it mostly depends on the t_{2g} states and it could be orbital-selective.

V. ACKNOWLEDGEMENTS

We acknowledge discussions with H. Tjeng. Calculations were done on the Jülich Blue Gene/P and Juropa. We acknowledge financial support from the Deutsche Forschungsgemeinschaft through research unit FOR1346.

- ¹ J. B. Goodenough, *J. Phys. Chem.Sol.* **6**, 287 (1958); P. M. Raccach and J. B. Goodenough, *Phys. Rev. B* **155**,932 (1967); J. B. Goodenough, *Mater. Res. Bull.* **6**, 967 (1971); M. A. Senaris-Rodriguez and J. B. Goodenough, *J. Solid State Chem.* **116**, 224 (1995).
- ² V. G. Bhide, D. S. Rajoria, G. Rama Rao, C. N. R. Rao, *Phys. Rev. B* **6**, 1021 (1972).
- ³ M. W. Haverkort, Z. Hu, J. C. Cezar, T. Burnus, H. Hartmann, M. Reuther, C. Zobel, T. Lorenz, A. Tanaka, N. B. Brookes, H. H. Hsieh, H.-J. Lin, C. T. Chen, and L. H. Tjeng, *Phys. Rev. Lett.* **97**, 176405 (2006).
- ⁴ A. Podlesnyak, S. Streule, J. Mesot, M. Medarde, E. Pomjakushina, K. Conder, A. Tanaka, M. W. Haverkort, and D. I. Khomskii, *Phys. Rev. Lett.* **97**, 247208 (2006).
- ⁵ N. Sundaram, Y. Jiang, I. E. Anderson, D. P. Belanger, C. H. Booth, F. Bridges, J. F. Mitchell, Th. Proffen, and H. Zheng, *Phys. Rev. Lett.* **102**, 026401 (2009).
- ⁶ G. Thornton, B. C. Tofield, and D. E. Williams, *Solid State Commun.* **44**, 1213 (1982); *J. Phys. Solid State Phys.* **21**, 2871 (1988).
- ⁷ K. Asai, P. Gehring, H. Chou, and G. Shirane, *Phys. Rev. B* **40**, 10982 (1989).
- ⁸ S. Yamaguchi, Y. Okimoto, H. Taniguchi, and Y. Tokura, *Phys. Rev. B* **53**, R2926 (1996).
- ⁹ R. H. Potze, G. A.Sawatzky, and M. Abbate, *Phys. Rev. B* **51**,11501 (1995).
- ¹⁰ T. Saitoh, T. Mizokawa, A. Fujimori, M. Abbate, Y. Takeda, M. Takano, *Phys. Rev. B* **55**, 4257 (1997).
- ¹¹ S. Noguchi, S. Kawamata, K. Okuda, H. Nojiri, and M. Motokawa, *Phys. Rev. B* **66**, 094404 (2002).
- ¹² M. A. Korotin, S. Yu. Ezhov, I. V. Solovyev, V. I. Anisimov, D. I. Khomskii, G. A. Sawatzky, *Phys. Rev. B* **54**, 5309 (1996).
- ¹³ R. F. Klie, J. C. Zheng and Y. Zhu, M. Varela, J. Wu and C. Leighton *Phys. Rev. Lett.* **99**, 047203 (2007).
- ¹⁴ C. Zobel, M. Kriener, D. Bruns, J. Baier, M. Grüninger, and T. Lorenz, P. Reutler and A. Revcolevschi, *Phys. Rev. B* **66**, 020402 (2002).
- ¹⁵ A. Ishikawa, J. Nohara and S. Sugai, *Phys. Rev. Lett.* **93**, 136401 (2004).
- ¹⁶ K. Asai, A. Yoneka, O. Yokokura, J.M. Tranquada, G. Shirane, and K. Kohn, *J. Phys. Soc. Japan* **67**, 290 (1998).
- ¹⁷ K. Knížek, Z. Jirák, J. Hejtmánek, P. Novák, and W. Ku, *Phys. Rev. B* **79**, 014430 (2009).
- ¹⁸ M. Zhuang, W. Zhang, N. Ming, *Phys. Rev. B* **57**, 10705 (1998).
- ¹⁹ K. Knížek, Z. Jirák, J. Hejtmánek and P. Novák, *J.Phys.: Condens. Matter* **18** 3285 (2006).
- ²⁰ A. Laref, and W. Sekkal, *Mat. Chem. Phys.* **123**, 125 (2010).
- ²¹ J. Kunes and V. Křápek, *Phys. Rev Lett.* **106**, 256401 (2011).
- ²² T. Kyomen, Y. Asaka, and M. Itoh, *Phys. Rev. B* **71**, 024418 (2005).
- ²³ T. Vogt, J. A. Hriljac, N. C. Hyatt, and P. Woodward, *Phys. Rev. B* **67**, R140401 (2003).
- ²⁴ R. Lengsdorf, J.-P. Rueff, G. Vankó, T. Lorenz, L. H. Tjeng, and M. M. Abd-Elmeguid, *Phys. Rev. B* **75**, 180401 (2007); R. Lengsdorf, M. Ait-Tahar, S. S. Saxena, M. Ellerby, D. I. Khomskii, H. Micklitz, T. Lorenz, and M. M. Abd-Elmeguid, *Phys. Rev. B* **69**, 140403 (2004).
- ²⁵ G. Vankó, J.-P. Rueff, A. Mattila, Z. Németh, and A. Shukla, *Phys. Rev. B* **73**, 024424 (2006).
- ²⁶ D. P. Kozlenko, N. O. Golosova, Z. Jirák, L. S. Dubrovinsky, B. N. Savenko, M. G. Tucker, Y. Le Godec, and V. P. Glazkov, *Phys. Rev. B* **75**, 064422 (2007).
- ²⁷ A. Mehta, R. Berliner and R. W. Smith, *J. Solid State Chem.* **130**,192 (1997); K. Knížek, Z. Jirák, J. Hejtmánek, M. Veverka, M. Maryško, B. C. Hauback, and H. Fjellvåg, *Phys. Rev. B* **73**, 214443 (2006).
- ²⁸ J.-Q. Yan, J.-S. Zhou, and J. B. Goodenough, *Phys. Rev. B* **69**, 134409 (2004).
- ²⁹ J. Baier, S. Jodlauk, M. Kriener, A. Reichl, C. Zobel, H. Kierspel, A. Freimuth, and T. Lorenz, *Phys. Rev. B* **71**, 014443 (2005).
- ³⁰ K. Knížek, Z. Jirák, J. Hejtmánek, M. Veverka, M. Maryško, G. Maris, and T.T.M. Palstra, *Eur. Phys. J* **47**, 213 (2005).
- ³¹ G. Thornton, B. C. Tofield, and A. W. Hewat, *J. Solid State Chem.* **61**, 301-307 (1986).
- ³² P. G. Radaelli and S.-W. Cheong, *Phys. Rev. B* **66**, 094408 (2002).
- ³³ S. Xu, Y. Morimoto, K. Mori, T. Kamiyama, T. Saitoh, A. Nakamura, *J. Phys. Soc. Jap.* **70**, 3296 (2001).
- ³⁴ G. Maris, Y. Ren, V. Volotchaev, C. Zobel, T. Lorenz, and T. T.M. Palstra, *Phys. Rev. B* **67**, 224423 (2003).
- ³⁵ D. Louca, J. L. Sarrao, J. D. Thompson, H. Röder, and G.H. Kwei, *Phys. Rev. B* **60**, 10378 (1999); D. Louca and J. L. Sarrao, *Phys. Rev. Lett.* **91**, 155501 (2003).
- ³⁶ R. Radwanski and Z. Ropka, *Solid State Commun.* **112**, 621 (1999); R. Radwanski and Z. Ropka, *Physica B* **281-282**, 507 (2000); Z. Ropka and R. Radwanski, *Phys. Rev. B* **67**, 172401 (2003).
- ³⁷ S. K. Pandey, A. Kumar, S. Patil, V. R. R. Medicherla, R. S. Singh, K. Maiti, D. Prabhakaran, A. T. Boothroyd, and A. V. Pimpale, *Phys. Rev. B* **77**, 045123 (2008).
- ³⁸ P. Blaha, K. Schwarz, G. Madsen, D. Kvasnicka and J. Luitz, WIEN2k, *An Augmented Plane Wave + Local Orbitals Program for Calculating Crystal Properties* (Karlheinz Schwarz, Techn. Universität Wien, Austria), 2001. ISBN 3-9501031-1-2.
- ³⁹ A. A. Mostofi, J.R. Yates, Y.-S. Lee, I. Souza, D. Vanderbilt, and N. Marzari, *Comp. Phys. Comm.* **178**, 685 (2008); J. Kunes, R. Arita, P. Wissgott, A. Toschi, H. Ikeda, and K. Held, *Comp. Phys. Comm.* **181**, 1888 (2010).
- ⁴⁰ E. Pavarini, S. Biermann, A. Poteryaev, A.I. Lichtenstein, A. Georges, O.K. Andersen, *Phys. Rev. Lett.* **92**, 176403 (2004); E. Pavarini, A. Yamasaki, J. Nuss and O. K. Andersen, *New J. Phys.* **7**, 188 (2005).
- ⁴¹ E. Pavarini, *The LDA+DMFT Approach*, in *The LDA+DMFT approach to strongly correlated materials* Verlag des Forschungszentrum Jülich, eds. E. Pavarini, E. Koch, A. Lichtenstein, D. Vollhardt (2011).
- ⁴² O. Gunnarsson, O. K. Andersen, O. Jepsen, J. Zaanen, *Phys. Rev. B* **39**, 1708 (1989).
- ⁴³ A.N. Rubtsov, V. V. Savkin, and A. I. Lichtenstein, *Phys. Rev. B* **72**, 035122 (2005).
- ⁴⁴ E. Pavarini, E. Koch, A.I. Lichtenstein, *Phys. Rev. Lett.* **101**, 266405 (2008); E. Pavarini and E. Koch, *Phys. Rev. Lett.* **104**, 086402 (2010); A. Flesch, G. Zhang, E. Koch, E. Pavarini, *Phys. Rev. B* **85**, 035124 (2012).
- ⁴⁵ E. Gorelov, M. Karolak, T.O. Wehling, F. Lechermann,

- A.I. Lichtenstein, E. Pavarini, Phys. Rev. Lett. **104**, 226401 (2010); M. Malvestuto, E. Carleschi, R. Fittipaldi, E. Gorelov, E. Pavarini, M. Cuoco, Y. Maeno, F. Parmigiani, A. Vecchione, Phys. Rev. B **83**,165121 (2011).
- ⁴⁶ A. S. Mishchenko, N. V. Prokof'ev, A. Sakamoto, and B. V. Svistunov, Phys. Rev. B **62**, 6317 (2000).
- ⁴⁷ In order to reduce the computational effort, most calculations are performed keeping only density-density terms; we find that differences due to the neglected terms are small in the relevant parameter regime.
- ⁴⁸ We find that the parameters depend very weakly on the position of RE $4f$ levels; we obtain very similar results if we treat f electrons within LDA+ U ($U \in [0, 7]$ eV), or if we replace RE $^{3+}$ with La $^{3+}$ (empty $4f$ shell).
- ⁴⁹ X. Liu and C. Prewitt, J. Phys. Chem. Solids **52**, 441 (1991); J. Pérez-Cacho, J. Blasco, J. García, and R. Sanchez, J. Solid State Chem. **150**, 145 (2000).
- ⁵⁰ R. Eder, Phys. Rev. **81** 035101 (2010).
- ⁵¹ T. Mizokawa and A. Fujimori, Phys. Rev. B **54**,5368 (1996).
- ⁵² E. Pavarini, S. C. Tarantino, T. B. Ballaran, M. Zema, P. Ghigna, P. Carretta, Phys. Rev. B **77**, 014425 (2008).
- ⁵³ J. A. Alonso, M. J. Martínez-Lope, C. de la Callea and V. Pomjakushin, J. Mater. Chem. **16**, 1555 (2006).
- ⁵⁴ K. Knížek, J. Hejtmánek, Z. Jiráček, P. Tomeš, P. Henry and G. André, Phys. Rev. B **79**, 134103 (2009).
- ⁵⁵ The crystal-field splittings obtained with the NMTO approach are slightly larger, but the trends remain the same. In the low-temperature ambient pressure phases $\Delta \sim 2.15$ eV while $\Delta \sim 2.4$ eV under a pressure of 8 GPa and ~ 2.05 eV at 900 K. For YCoO $_3$ we find ~ 2.15 eV at 300 K and 2.0 at ~ 900 K. The change in crystal-field splitting between high-spin and low spin phases is in all cases at most 300 meV.
- ⁵⁶ For $3d$ elements, the ratio F_4/F_2 is usually approximated to ~ 0.625 ; this yields $\Delta\mathcal{J}_{\text{avg}}/\mathcal{J}_{\text{avg}} \sim 0.08$. The extreme values for $\Delta\mathcal{J}_{\text{avg}}/\mathcal{J}_{\text{avg}}$ are 0 ($F_4 = F_2$) and 0.2 ($F_4 = 0$).
- ⁵⁷ B N.Figgis, M. A. Hitchman, in *Ligand Field Theory and its Applications*, Wiley, New York (2000).
- ⁵⁸ G. Thornton, F. C. Morrison, S. Partington, B. C. Tofield, D. E. Williams, J. Phys. C: Solid State Phys. **21**, 2871 (1988); K. Knížek, Z. Jiráček, J. Hejtmánek, M. Veverka, M. Maryško, G. Maris, and T.T. M. Palstra, Eur. Phys. J. B **47**, 213 (2005).
- ⁵⁹ M. De Raychaudhury, E. Pavarini and O.K. Andersen, Phys. Rev. Lett. **99**, 126402 (2007).
- ⁶⁰ T. Mizokawa and A. Fujimori, Phys. Rev. B **54**, 5368 (1996).
- ⁶¹ M. Takahashi and J-I. Igarashi, Phys. Rev. B **55**, 13557 (1997).
- ⁶² H. Hsu, K. Umemoto, M. Cococcioni, R. Wentzcovitch, Phys. Rev. B **79**, 125124 (2009).
- ⁶³ A. Chainani, M. Mathew, and D. D. Sarma, Phys. Rev. B **46**, 9976 (1992).
- ⁶⁴ C.S. Naiman, R. Gilmore, B. DiBartolo, A. Linz, and R. Santoro, J. Appl. Phys. **36**, 1044 (1965).
- ⁶⁵ We find that, for \mathcal{J}_{avg} between 0 and 1 eV, the superexchange energy gain is reduced of about 30 meV for $S = 2$ and increased of about the same amount for $S = 0$; the trends remain the same.
- ⁶⁶ The IS state could be included in our model as a third excited state. In this case instead of a Ising model for a pseudospin 1/2, we would obtain an Ising model for a pseudospin 1.
- ⁶⁷ Y. Tokura, Y. Okimoto, S. Yamaguchi, H. Taniguchi, T. Kimura and H. Takagi, Phys. Rev. B **58**, 1699 (1998).
- ⁶⁸ To reduce the sign problem we dropped Coulomb terms without a density-density matrix form; this moves the spin-state transition to slightly larger values of Δ_{LH} ($2.8\mathcal{J}_{\text{avg}}$ versus $2.6\mathcal{J}_{\text{avg}}$), as discussed in section II A, but do not affects the conclusions.
- ⁶⁹ O. Gunnarsson, E. Koch and R.M. Martin, Phys. Rev. B **56**, 1146 (1997); E. Koch, O. Gunnarsson, and R. M. Martin, Phys. Rev. B **60**, 15714 (1999).
- ⁷⁰ A. G. Thomas, W. R. Flavell, P. M. Dunwoody, C.E.J. Mitchell, S. Warren, S. C. Grice, P.G.D Marr, D. E. Jewitt, N. Khan, V.R. Dhanak, D. Teehan, E.A. Seddon, K. Asai, Y. Koboyashi and N. Yamada, J. Phys.: Condens. Matter **12**, 9259 (2000).
- ⁷¹ M. Medarde, C. Dallera, M. Grioni, J. Voigt, A. Podlesnyak, E. Pomjakushina, K. Conder, Th. Neisius, O. Tjénberg, and S.N. Barilo, Phys. Rev. B **73**, 054424 (2006).